Spin-ordering and magnon collective modes for two-dimensional electron lattices in strong magnetic fields

R. Côté

Département de Physique et Centre de Recherches en Physique du Solide, Université de Sherbrooke, Sherbrooke, Québec, Canada J1K-2R1

A. H. MacDonald

Department of Physics, Indiana University, Bloomington, Indiana 47405

We study the spin-ordering and the magnon collective modes of the two-dimensional Wigner crystal state at strong magnetic fields. Our work is based on the Hartree-Fock approximation for the ground state and the time-dependent Hartree-Fock approximation for the collective modes. We find that the ground state is ferromagnetic, i.e., that all spins are aligned at $T=0$ even when the electronic g factor is negligibly small. The magnon calculations show that the spin stiffness is much smaller in the crystal state than in fluid states which occur at nearby Landau-level filling factors.

I. INTRODUCTION

At sufficiently low electron densities or in sufficiently strong magnetic fields, electrons will crystallize at low temperatures.[1,2] It is generally expected that in the (Wigner) crystal state, electronic spins will be either ferromagnetically or antiferromagnetically ordered.[3,4] There has long been theoretical interest[5,6] in the rather subtle physics which determines how the electronic spins are ordered. For two-dimensional electrons in the Wigner crystal state at zero magnetic field a series[7,8] of variational and Green's function Monte Carlo calculations have not led to definitive conclusions concerning the nature of the magnetic order. The energetically preferred spin ordering has been shown to depend very much on the lattice structure of the electron crystal and, unfortunately, the difference in energy between states with different spin order on a hexagonal lattice (which is expected to be the ground-state lattice of the Wigner crystal) is smaller than the accuracy of the Monte Carlo calculations.[8] To our knowledge, there are no previous numerical studies of the spin structure of the Wigner crystal in the strong-field regime. The variational Monte Carlo calculations cited above considered, in the strong-field limit, only the spin-polarized hexagonal lattice and investigated exchange, correlation, and Landau-level-mixing effects.[8]

In this paper we discuss magnetic order for two-dimensional electrons in the limit of strong perpendicular magnetic fields where all electrons are confined to the lowest quantized kinetic energy Landau level. In this limit, the state of the electrons depends on the Landau-level filling factor ν rather than the electron density and, except for a narrow interval surrounding $\nu=0.2$, the electrons form a Wigner crystal state[2] for ν smaller than ≈ 0.23. [$\nu \equiv N/N_\phi$ where N is the number of electrons and $N_\phi = SB/\Phi_0 \equiv S/(2\pi l^2)$ is the Landau-level degeneracy. Here S is the area of the system, B is the magnetic field strength, l is the magnetic length, and $\Phi_0 = hc/e$ is the magnetic flux quantum.] We find, partly on the basis of Hartree-Fock approximation

(HFA) calculations, that in this regime the Wigner crystal state will always be ferromagnetic. The Hartree-Fock ground-state wave function does not contain the important correlations that give rise to the magnetophonon and spin-wave modes of the crystal. We can check, however, the stability of the spin-polarized lattice by evaluating the magnon spectrum of the Wigner crystal using a time-dependent Hartree-Fock approximation (TDHFA). Within the limits of our numerical approach, we find that the polarized lattices remain stable at small filling factors. Moreover, in this limit, the spin-wave modes are very well described by a Heisenberg model where electrons are localized on their lattice site with an effective exchange integral J_{TDHFA} that we compute for different filling factors. From the value of this effective exchange integral, we can derive the spin stiffness of the Wigner crystal state and compare its value with the spin stiffness of ferromagnetic electron fluid states at nearby filling factors. This comparison shows that the spin stiffness of the liquid is much larger than that of the solid. This is so because the exchange energy is larger when the electrons are free to move around and come closer to each other.

Our paper is organized as follows. In Sec. II we outline the formalism we use to perform the HFA and TDHFA calculations for, respectively, the ground state and spin waves of the system. We are able to enormously simplify the calculations by adapting an approach we developed[9] previously to the situation of interest here. In Sec. III we present numerical results for the magnetic ground state of the square and triangular Wigner crystal states and discuss differences between magnetic-ordering tendencies in zero-field and strong-field limits. Our results for magnon dispersion relation are presented and discussed in Sec. IV. Section V contains a brief summary of this work.

II. HARTREE-FOCK AND TIME-DEPENDENT HARTREE-FOCK APPROXIMATIONS

A. Hartree-Fock approximation ground state

The formalism outlined in this section is a straightforward generalization of one which we developed originally[9] to de-

    <u>53</u>   10 019

scribe phonon modes in the Wigner crystal state, and which has previously been generalized in other directions[10,11] to describe double-layer quantum Hall systems and edge excitations of the Wigner crystal. We outline the main steps in the development of the formalism and refer the reader to Ref. 9 for further details.

We consider a two-dimensional electron gas (2DEG) in a magnetic field $\mathbf{B} = -B\hat{\mathbf{z}}$ which is assumed to be strong enough so that we can make the usual approximation of considering only the lowest Landau level. In the Landau gauge, the Hamiltonian of the 2DEG is then (we set $\hbar = 1$ throughout this paper)

$$
\begin{aligned}
H = \sum_{\alpha,X} \epsilon_\alpha c^\dagger_{\alpha,X} c_{\alpha,X} + \frac{1}{2S} \sum_{\mathbf{q}} \sum_{X_1,\ldots,X_4} \sum_{\alpha,\beta} V(\mathbf{q}) \\
\times \langle X_1 | \exp(i\mathbf{q}\cdot\mathbf{r}) | X_4 \rangle \langle X_2 | \exp(-i\mathbf{q}\cdot\mathbf{r}) | X_3 \rangle \\
\times c^\dagger_{\alpha,X_1} c^\dagger_{\beta,X_2} c_{\beta,X_3} c_{\alpha,X_4},
\end{aligned} \tag{1}
$$

where $\alpha, \beta = +$ (up), $-$ (down) are spin indices and the lowest Landau level has the energy

$$
\epsilon_\alpha = \frac{\omega_c}{2} - \frac{\alpha g^* \mu_b B}{2}. \tag{2}
$$

As usual, $\omega_c = eB/m^*c$ is the cyclotron frequency and m^* and g^* are the effective mass and g factor of the electron appropriate to the two-dimensional electron layer.[4] For a finite system, the allowed values of the quantum number X are separated by $2\pi l^2/L_y$. Neglecting the finite thickness of the two-dimensional electron layer, we take $V(\mathbf{q}) = 2\pi e^2/q$, the two-dimensional Fourier transform of the Coulomb potential.

Making the usual Hartree-Fock pairing of the second-quantized operators in the Hamiltonian of Eq. (1) and allowing for the possibility of broken translational symmetry and spin magnetic order in the ground state, we obtain

$$
H = N_\phi \sum_\alpha \epsilon_\alpha \rho_{\alpha,\alpha}(0) + N_\phi \sum_{\mathbf{q}} \sum_{\alpha,\beta} V_{\alpha,\beta}(\mathbf{q}) \rho_{\alpha,\beta}(\mathbf{q}), \tag{3}
$$

where we have introduced the operators

$$
\rho_{\alpha,\beta}(\mathbf{q}) = N_\phi^{-1} \sum_X \exp(-iq_x X - iq_x q_y l^2/2) c^\dagger_{\alpha,X} c_{\beta,X+q_y l^2}, \tag{4}
$$

which are related to the density and spin operators by the relations

$$
n(q) = N_\phi e^{-q^2 l^2/4} [\rho_{++}(\mathbf{q}) + \rho_{--}(\mathbf{q})],
$$

$$
S^z(q) = \frac{1}{2} N_\phi e^{-q^2 l^2/4} [\rho_{++}(\mathbf{q}) - \rho_{--}(\mathbf{q})],
$$
(5)

$$
S^+(q) = N_\phi e^{-q^2 l^2/4} \rho_{+-}(\mathbf{q}),
$$

$$
S^-(q) = N_\phi e^{-q^2 l^2/4} \rho_{-+}(\mathbf{q}).
$$

The matrix elements of the Hartree-Fock self-consistent field in Eq. (3) are given by

$$
V_{++}(\mathbf{q}) = [H(\mathbf{q}) - X(\mathbf{q})] \langle \rho_{++}(-\mathbf{q}) \rangle + H(\mathbf{q}) \langle \rho_{--}(-\mathbf{q}) \rangle,
$$

$$
V_{--}(\mathbf{q}) = [H(\mathbf{q}) - X(\mathbf{q})] \langle \rho_{--}(-\mathbf{q}) \rangle + H(\mathbf{q}) \langle \rho_{++}(-\mathbf{q}) \rangle,
$$
(6)

$$
V_{+-}(\mathbf{q}) = -X(\mathbf{q}) \langle \rho_{-+}(-\mathbf{q}) \rangle,
$$

$$
V_{-+}(\mathbf{q}) = -X(\mathbf{q}) \langle \rho_{+-}(-\mathbf{q}) \rangle,
$$

with the Hartree (H) and Fock (X) interactions defined by

$$
H(\mathbf{q}) = \left(\frac{e^2}{l}\right)\left(\frac{1}{ql}\right) e^{-q^2 l^2/2}(1 - \delta_{\mathbf{q},0}),
$$

$$
X(\mathbf{q}) = \left(\frac{e^2}{l}\right) \sqrt{\frac{\pi}{2}} e^{-q^2 l^2/4} I_0(q^2 l^2/4), \tag{7}
$$

where $I_0(x)$ is the modified Bessel function of the first kind and the factor $(1 - \delta_{\mathbf{q},0})$ comes from the neutralizing positive background.

The ordered state is defined by the set of order parameters $\{\langle \rho_{\alpha,\beta}(\mathbf{q}) \rangle\}$. In the case of interest here, i.e., for a Wigner lattice, these parameters are nonzero only when $\mathbf{q} = \mathbf{G}$, a reciprocal lattice vector of the crystal. To calculate the $\langle \rho_{\alpha,\beta}(\mathbf{q}) \rangle$'s, we define the 2×2 single-particle Green's function

$$
G_{\alpha,\beta}(X,X',\tau) = -\langle T c_{\alpha,X}(\tau) c^\dagger_{\beta,X'}(0) \rangle \tag{8}
$$

and its Fourier transform $G_{\alpha,\beta}(\mathbf{q},\tau)$ by

$$
\begin{aligned}
G_{\alpha,\beta}(\mathbf{q},\tau) = N_\phi^{-1} \sum_{X,X'} G_{\alpha,\beta}(X,X',\tau) \\
\times \exp\left[-\frac{1}{2} i q_x (X+X')\right] \delta_{X',X-q_y l^2},
\end{aligned} \tag{9}
$$

so that

$$
\langle \rho_{\alpha,\beta}(\mathbf{q}) \rangle = G_{\beta,\alpha}(\mathbf{q}, \tau = 0^-). \tag{10}
$$

Using the Heisenberg equation of motion $(\partial/\partial\tau) \times (\cdots) = [H - \mu N, (\cdots)]$ where μ is the chemical potential of the electrons which we measure with respect to the kinetic energy of the first Landau level, we obtain the equation of motion for the single-particle Green's function (in an obvious matrix notation):

$$
\begin{aligned}
\left[(i\omega_n + \mu)I - \Lambda \begin{pmatrix} 1 & 0 \\ 0 & -1 \end{pmatrix}\right] G(\mathbf{q},\omega_n) - \sum_{\mathbf{q}'} \exp\left[\frac{1}{2} i\mathbf{q} \times \mathbf{q}' l^2\right] \\
\times V(\mathbf{q}' - \mathbf{q}) G(\mathbf{q}', \omega_n) = I\delta_{\mathbf{q},0},
\end{aligned} \tag{11}
$$

where ω_n is a fermionic Matsubara frequency, $\Lambda \equiv g^* \mu_b B/2$, and I is the 2×2 unit matrix. G and V are the 2×2 matrices defined in Eqs. (8) and (6).

Equation (11) is very general. For example, it can be used to consider complex spin-texture states such as the Skyrme crystal studied in Ref. 10, where the average values of all three components of the average spin are space dependent. Although we concentrate, in this work, on simple spin-structure states where Eq. (11) can be reduced to only one uncoupled equation, we explain here our numerical approach for the general case.

We represent by $\mathbf{q}_1, \mathbf{q}_2, \mathbf{q}_3, \ldots, \mathbf{q}_N$ the wave vectors defining the ordered state (in principle, $N \to \infty$ but in the numerical calculation, a suitable cutoff is chosen for N). We choose $\mathbf{q}_1 = 0$ and define the vector $\tilde{G}_{\alpha,\beta} \equiv (G_{\alpha,\beta}(\mathbf{q}_1), G_{\alpha,\beta}(\mathbf{q}_2), G_{\alpha,\beta}(\mathbf{q}_3), \ldots, G_{\alpha,\beta}(\mathbf{q}_N))$. Since in Eq. (11), G_{++} (or G_{--}) is coupled to G_{-+} (or G_{+-}) only, we can simplify Eq. (11) by defining the $2N$-component vectors $\tilde{G}_1 \equiv (\tilde{G}_{++}, \tilde{G}_{-+})$ and $\tilde{G}_2 \equiv (\tilde{G}_{+-}, \tilde{G}_{--})$. We finally get a set of two coupled integral equations that we write in matrix form as

$$(i\omega_n + \mu)\tilde{I} \begin{pmatrix} \tilde{G}_{++} \\ \tilde{G}_{-+} \end{pmatrix} - \tilde{F} \begin{pmatrix} \tilde{G}_{++} \\ \tilde{G}_{-+} \end{pmatrix} = \begin{pmatrix} \tilde{I} \\ \tilde{0} \end{pmatrix}, \qquad (12)$$

and

$$(i\omega_n + \mu)\tilde{I} \begin{pmatrix} \tilde{G}_{+-} \\ \tilde{G}_{--} \end{pmatrix} - \tilde{F} \begin{pmatrix} \tilde{G}_{+-} \\ \tilde{G}_{--} \end{pmatrix} = \begin{pmatrix} \tilde{0} \\ \tilde{I} \end{pmatrix}. \qquad (13)$$

In these equations, $\tilde{I}$ is the $2N \times 2N$ unit matrix, $\tilde{I} \equiv (1,0,0,\ldots,0)$ and $\tilde{0} \equiv (0,0,0,\ldots,0)$ are, respectively, the N-component unit and null vectors, and $\tilde{F}$ is the $2N \times 2N$ matrix defined by

$$\tilde{F} \equiv \begin{bmatrix} \Lambda \delta_{\mathbf{q},\mathbf{q}'} + A_{++}(\mathbf{q},\mathbf{q}') & A_{+-}(\mathbf{q},\mathbf{q}') \\ A_{-+}(\mathbf{q},\mathbf{q}') & -\Lambda \delta_{\mathbf{q},\mathbf{q}'} + A_{--}(\mathbf{q},\mathbf{q}') \end{bmatrix}, \qquad (14)$$

where

$$A_{\alpha,\beta}(\mathbf{q},\mathbf{q}') = \exp\left[\frac{1}{2} i\mathbf{q} \times \mathbf{q}' l^2\right] V_{\alpha,\beta}(\mathbf{q}' - \mathbf{q}). \qquad (15)$$

Note that since $A_{\alpha,\beta}(\mathbf{q},\mathbf{q}') = [A_{\beta,\alpha}(\mathbf{q}',\mathbf{q})]^*$, $\tilde{F}$ is a Hermitian matrix. It follows that Eqs. (12) and (13) can be solved by making the unitary transformation $\tilde{F} = UDU^\dagger$, where $UU^\dagger = 1$ and D is the diagonal matrix containing the eigenvalues of $\tilde{F}$. Following Ref. 9, we have for the order parameters ($i = 1, 2, \ldots, N$)

$$\langle \rho_{++}(\mathbf{q}_i) \rangle = \sum_{k=1}^{k=k_{\max}} U_{i,k} U_{1,k}^*,$$

$$\langle \rho_{+-}(\mathbf{q}_i) \rangle = \sum_{k=1}^{k=k_{\max}} U_{i+N,k} U_{1,k}^*,$$

$$\langle \rho_{-+}(\mathbf{q}_i) \rangle = \sum_{k=1}^{k=k_{\max}} U_{i,k} U_{N+1,k}^*,$$

$$\langle \rho_{--}(\mathbf{q}_i) \rangle = \sum_{k=1}^{k=k_{\max}} U_{i+N,k} U_{N+1,k}^*.$$

The value of $k_{\max}$ is obtained from the conditions

$$\langle \rho_{++}(0) \rangle = \nu_+ \qquad (17)$$

and

$$\langle \rho_{--}(0) \rangle = \nu_-, \qquad (18)$$

the filling factors for spin up and down. It is easy to show from Eq. (16) that, at $T = 0$ K, the following sum rules hold:

$$\sum_{\mathbf{q}} [|\langle \rho_{++}(\mathbf{q}) \rangle|^2 + |\langle \rho_{+-}(\mathbf{q}) \rangle|^2] = \nu_+, \qquad (19)$$

and

$$\sum_{\mathbf{q}} [|\langle \rho_{-+}(\mathbf{q}) \rangle|^2 + |\langle \rho_{--}(\mathbf{q}) \rangle|^2] = \nu_-. \qquad (20)$$

We note that, except for simple cases such as fully polarized or unpolarized crystals, the filling factors ν_+ and ν_- are not known from the beginning. The only boundary conditions are the constraints

$$\langle \rho_{++}(0) \rangle + \langle \rho_{--}(0) \rangle = \nu \qquad (21)$$

and

$$\langle \rho_{+-}(0) \rangle = \langle \rho_{-+}(0) \rangle = 0 \quad \text{if} \ \Lambda \neq 0. \qquad (22)$$

Also, by definition,

$$\langle \rho_{+-}(\mathbf{q}) \rangle = \langle \rho_{-+}(-\mathbf{q}) \rangle^*. \qquad (23)$$

To find ν_+ and ν_-, Eqs. (12) and (13) must be solved self-consistently for given values of ν_+ and ν_- until a convergent solution is obtained. The process has to be repeated for different sets of ν_+ and ν_- values until the lowest-energy solution is found. In this way we can determine the lowest-energy single Slater determinant consistent with any assumed translational and magnetic symmetry. The Hartree-Fock energy per particle of a particular ground-state configuration (with respect to the kinetic energy of the lowest Landau level) is

$$E = \Lambda \left(\frac{\nu_- - \nu_+}{\nu} \right) + \frac{1}{2\nu} \sum_{\mathbf{q}} \ \{ [H(\mathbf{q}) - X(\mathbf{q})][|\langle \rho_{++}(\mathbf{q}) \rangle|^2$$

$$+ |\langle \rho_{--}(\mathbf{q}) \rangle|^2] + H(\mathbf{q})[\langle \rho_{++}(\mathbf{q}) \rangle \langle \rho_{--}(-\mathbf{q}) \rangle + \text{H.c.}]$$

$$- 2X(\mathbf{q})|\langle \rho_{+-}(\mathbf{q}) \rangle|^2 \}. \tag{24}$$

In the case of a fully spin-polarized Wigner crystal, only $\{\langle \rho_{++}(\mathbf{G}) \rangle\} \neq 0$ ($\mathbf{G}$ is a reciprocal lattice vector) and Eq. (11) simplifies to

$$(i\omega_n + \mu - \Lambda)G_{++}(\mathbf{G}, \omega_n) - \sum_{\mathbf{G}'} \tilde{F}(\mathbf{G}, \mathbf{G}')G_{++}(\mathbf{G}', \omega_n)$$

$$= \delta_{\mathbf{G},0}, \tag{25}$$

where $\tilde{F}$ is now the $N \times N$ matrix

$$\tilde{F}(\mathbf{G}, \mathbf{G}') = \exp \left[\frac{1}{2} i \mathbf{G} \times \mathbf{G}' l^2 \right] V_{++}(\mathbf{G} - \mathbf{G}'), \tag{26}$$

with

$$V_{++}(\mathbf{G}) = [H(\mathbf{G}) - X(\mathbf{G})]\langle \rho_{++}(\mathbf{G}) \rangle. \tag{27}$$

The ground-state energy per particle, in this case, is simply

$$E_{++} = -\Lambda + \frac{1}{2\nu} \sum_{\mathbf{G}} \ [H(\mathbf{G}) - X(\mathbf{G})]|\langle \rho_{++}(\mathbf{G}) \rangle|^2. \tag{28}$$

B. Time-dependent Hartree-Fock approximation collective excitations

To determine the collective excitation energies of the ordered state, we define the response functions

$$\chi_{\alpha\beta\gamma\delta}(\mathbf{q}, \mathbf{q}'; \tau) = -g \langle T \tilde{\rho}_{\alpha\beta}(\mathbf{q}, \tau) \tilde{\rho}_{\gamma\delta}(-\mathbf{q}', 0) \rangle, \tag{29}$$

where $\tilde{\rho}_{\alpha\beta} = \rho_{\alpha\beta} - \langle \rho_{\alpha\beta} \rangle$. By making use of the commutation relation[9] of the operators $\rho_{\alpha\beta}(\mathbf{q})$ and of the HF Hamiltonian of Eq. (3), we obtain an equation of motion for the response functions that corresponds to the HFA which we denote by χ^0. We get (repeated spin indices are summed over)

$$[i\Omega_n + (\epsilon_\alpha - \epsilon_\beta)]\chi^0_{\alpha\beta\gamma\delta}(\mathbf{q}, \mathbf{q}'; \Omega_n) = \delta_{\beta,\gamma} e^{-i\mathbf{q} \times \mathbf{q}' l^2/2} \langle \rho_{\alpha\delta}(\mathbf{q} - \mathbf{q}') \rangle - \delta_{\alpha,\delta} e^{i\mathbf{q} \times \mathbf{q}' l^2/2} \langle \rho_{\gamma\beta}(\mathbf{q} - \mathbf{q}') \rangle - \sum_{\mathbf{q}''} V_{\kappa\alpha}(\mathbf{q}'' - \mathbf{q}) e^{-i\mathbf{q} \times \mathbf{q}'' l^2/2}$$

$$\times \chi^0_{\kappa\beta\gamma\delta}(\mathbf{q}'', \mathbf{q}'; \Omega_n) + \sum_{\mathbf{q}''} V_{\beta\kappa}(\mathbf{q}'' - \mathbf{q}) e^{i\mathbf{q} \times \mathbf{q}'' l^2/2} \chi^0_{\alpha\kappa\gamma\delta}(\mathbf{q}'', \mathbf{q}', \Omega_n), \tag{30}$$

where Ω_n is a boson frequency.

To calculate the response functions in the time-dependent Hartree-Fock approximation (TDHFA), and so include the correlations that give rise to phonons and magnons, we need to sum a set of ladder and bubble diagrams.[9] The final equation for χ can be expressed *solely* in terms the order parameters of the crystal phase,

$$\chi_{\alpha\beta\gamma\delta}(\mathbf{q}, \mathbf{q}'; \Omega_n) = \tilde{\chi}_{\alpha\beta\gamma\delta}(\mathbf{q}, \mathbf{q}'; \Omega_n) + \sum_{\mathbf{q}''} \tilde{\chi}_{\alpha\beta\kappa\kappa}(\mathbf{q}, \mathbf{q}''; \Omega_n)$$

$$\times H(\mathbf{q}'')\chi_{\xi\xi\gamma\delta}(\mathbf{q}'', \mathbf{q}'; \Omega_n), \tag{31}$$

where the irreducible response function is given by

$$\tilde{\chi}_{\alpha\beta\gamma\delta}(\mathbf{q}, \mathbf{q}'; \Omega_n) = \chi^0_{\alpha\beta\gamma\delta}(\mathbf{q}, \mathbf{q}'; \Omega_n) - \sum_{\mathbf{q}''} \chi^0_{\alpha\beta\kappa\xi}(\mathbf{q}, \mathbf{q}''; \Omega_n)$$

$$\times X(\mathbf{q}'')\tilde{\chi}_{\xi\kappa\gamma\delta}(\mathbf{q}'', \mathbf{q}'; \Omega_n). \tag{32}$$

The spin and density response functions are obtained, as usual, from the analytic continuation $i\Omega_n \rightarrow \omega + i\delta$. The dispersion relation of the collective modes are then found by tracking the poles of the response functions at different values of the wave vector $\mathbf{q}$ in the Brillouin zone.

In the case of a fully polarized state, the only nonzero response functions are χ_{+--+}, χ_{-++-}, and χ_{++++} and so the usual spin-flip and density-density response functions are given by

$$\chi^{+-}(\mathbf{q}, \mathbf{q}'; \Omega_n) = g e^{-q^2 l^2/4} e^{-q'^2 l^2/4} \chi_{+--+}(\mathbf{q}, \mathbf{q}'; \Omega_n) \tag{33}$$

and

$$\chi^{zz}(\mathbf{q}, \mathbf{q}'; \Omega_n) = \frac{1}{4} \chi^{nn}(\mathbf{q}, \mathbf{q}'; \Omega_n)$$

$$= \frac{g}{4} e^{-q^2 l^2/4} e^{-q'^2 l^2/4} \chi_{++++}(\mathbf{q}, \mathbf{q}'; \Omega_n). \tag{34}$$

They obey the TDHFA equations of motion

$$\sum_{\mathbf{q}''} \ \{ i\Omega_n \delta_{\mathbf{q}, \mathbf{q}''} - C_A(\mathbf{q}, \mathbf{q}'') - D_A(\mathbf{q}, \mathbf{q}'')[H(\mathbf{q}'') - X(\mathbf{q}'')] \}$$

$$\times \chi_{++++}(\mathbf{q}'', \mathbf{q}'; \Omega_n) = D_A(\mathbf{q}, \mathbf{q}') \tag{35}$$

and

$$\sum_{\mathbf{q}''}[(i\Omega_n-2\Lambda)\delta_{\mathbf{q},\mathbf{q}''}-C_B(\mathbf{q},\mathbf{q}'')+D_B(\mathbf{q},\mathbf{q}'')X(\mathbf{q}'')]$$

$$\times\chi_{+--+}(\mathbf{q}'',\mathbf{q}';\Omega_n)=D_B(\mathbf{q},\mathbf{q}'),\qquad(36)$$

where we have defined

$$D_A(\mathbf{q},\mathbf{q}')=-2i\,\sin[(\mathbf{q}\times\mathbf{q}')l^2/2],\qquad(37)$$

$$D_B(\mathbf{q},\mathbf{q}')=\langle\rho_{++}(\mathbf{q}-\mathbf{q}')\rangle e^{-i(\mathbf{q}\times\mathbf{q}')l^2/2},\qquad(38)$$

$$C_A(\mathbf{q},\mathbf{q}')=2i\langle\rho_{++}(\mathbf{q}-\mathbf{q}')\rangle[H(\mathbf{q}-\mathbf{q}')-X(\mathbf{q}-\mathbf{q}')]$$
$$\times\sin[(\mathbf{q}\times\mathbf{q}')l^2/2],\qquad(39)$$

$$C_B(\mathbf{q},\mathbf{q}')=\langle\rho_{++}(\mathbf{q}-\mathbf{q}')\rangle X(\mathbf{q}-\mathbf{q}')\cos[(\mathbf{q}\times\mathbf{q}')l^2/2]$$
$$+\langle\rho_{++}(\mathbf{q}-\mathbf{q}')\rangle[2iH(\mathbf{q}-\mathbf{q}')-iX(\mathbf{q}-\mathbf{q}')]$$
$$\times\sin[(\mathbf{q}\times\mathbf{q}')l^2/2].\qquad(40)$$

(For a Wigner crystal, $\mathbf{q}\to\mathbf{k}+\mathbf{G}$, $\mathbf{q}'\to\mathbf{k}+\mathbf{G}'$, etc., where $\mathbf{k}$ is a vector restricted to the first Brillouin zone of the crystal.) The problem of calculating the spin-flip and density-density response functions is then reduced to a matrix-diagonalization problem. The two response functions decouple. The matrix eigenvalues are the collective excitations associated with the two response functions, phonons in the case of χ^{nn} and magnons in the case of χ^{+-}.

III. HARTREE-FOCK APPROXIMATION FOR THE GROUND STATE

We first apply the above formalism to examine the nature of the magnetic order in the Wigner crystal ground state. In the Hartree-Fock approximation the ground state at strong magnetic fields always has broken translational symmetry.[13] This result of the Hartree-Fock approximation is an artifact. As we mentioned in the Introduction, the true ground state has broken translational symmetry only for $\nu<0.23$.[14] Nevertheless, as we discuss further below, the Hartree-Fock approximation does describes *the ground state* reasonably accurately when the ground state *is* a Wigner crystal. Of course the Hartree-Fock approximation completely misrepresents the excitation spectrum of the Wigner crystal, since it misses the phonon and magnon collective modes captured by the time-dependent Hartree-Fock approximation.

In two dimensions, Coulomb interactions favor a triangular lattice for the Wigner crystal.[12] We will find that the energy scale associated with magnetic order is much smaller than the Coulomb energy scale. We therefore expect the structure of the Wigner crystal to be the triangular lattice structure dictated by Coulomb interactions. We also expect that the interactions between the spins on the triangular lattice sites will be predominantly nearest neighbor since the overlap between wave functions on different sites is quite small in a strong magnetic field. We check this approxima-

tion below by comparing the dispersion relation of the spin waves in the TDHFA with that given by a Heisenberg model with only nearest-neighbor exchange coupling. The ground state for two-dimensional spin-1/2 particles with nearest-neighbor interactions on a triangular lattice is expected to have long range order for both ferromagnetic and antiferromagnetic interactions.[15] However, because of frustration, the order is rather subtle for the antiferromagnetic case. (The triangular lattice is *not* a bipartite lattice.) Our primary objective in this subsection is to determine whether the interaction is ferromagnetic or antiferromagnetic by comparing the energy of these two states. For that purpose it is more useful to consider the case of two-dimensional electrons on a square lattice since it is bipartite and both antiferromagnetic and ferromagnetic states have a simple structure. We do so even though the ground state of the two-dimensional electron solid does not occur in this structure.

A. Maki-Zotos wave function

It is instructive to begin by generalizing the wave function for spinless electrons employed by Maki and Zotos[16] in their study of the strong-field Wigner crystal. We define

$$\Psi=(N!)^{-1/2}\det|\psi_{\mathbf{R}_j}(\mathbf{r}_i)\chi_{\mathbf{n}_j}^i|.\qquad(41)$$

Here $\mathbf{R}_j$ is the jth lattice vector,

$$\psi_{\mathbf{R}}(\mathbf{r})=\frac{1}{\sqrt{2\pi l^2}}\exp\left(\frac{-|\mathbf{r}-\mathbf{R}|^2-2i(xR_y-yR_x)}{4l^2}\right),\quad(42)$$

is the lowest-Landau-level wave function[17] for an electron whose quantized cyclotron orbit is centered on $\mathbf{R}$, and $\chi_{\mathbf{n}}=(\cos(\theta/2),\sin(\theta/2)\exp(i\phi))$ is a spinor oriented in the $\mathbf{n}=(\sin(\theta)\cos(\phi),\sin(\theta)\sin(\phi),\cos(\theta))$ direction. In this wave function the cyclotron orbits of electrons near different lattice sites are uncorrelated and the electron spin orientation at a given lattice site is arbitrary. In the range of ν where the ground state is a Wigner crystal it is an excellent approximation[16,18] to ignore the lack of orthogonality between cyclotron orbits centered at different lattice sites. Making this approximation, it is easy to derive an expression for

$$E\equiv\frac{\langle\Psi|\Sigma_{i<j}e^2|\mathbf{r}_i-\mathbf{r}_j|^{-1}|\Psi\rangle}{\langle\Psi|\Psi\rangle}.\qquad(43)$$

In Eq. (43), we have dropped the Zeeman energy, which can easily be added if the electronic g factor is nonzero. The fact that the kinetic energy, taken as the zero of energy above, is quantized is important in determining the favored magnetic order. Following Maki and Zotos we find that

$$E=\frac{1}{2}\sum_{i\neq j}\left[I(|\mathbf{R}_j-\mathbf{R}_i|)-\left(\frac{1+\mathbf{n}_i\cdot\mathbf{n}_j}{2}\right)J_{\text{MZ}}(|\mathbf{R}_j-\mathbf{R}_i|)\right],$$
$$(44)$$

where

$$I(R) = \left(\frac{e^2}{l}\right) \frac{\sqrt{\pi}}{2} \exp(-R^2/8l^2) I_0(R^2/8l^2) \qquad (45)$$

and

$$J_{MZ}(R) = \exp(-R^2/4l^2) I(R). \qquad (46)$$

In this equation $I(R)$ and $J(R)$ are, respectively, the direct and exchange two-body matrix elements of the Coulomb interaction for lowest-Landau-level cyclotron orbits whose centers are separated by $\mathbf{R}$. The explicit expression for the matrix element in the exchange term, which is sensitive to the relative orientations of the spins on the two sites, is

$$J_{MZ}(|\mathbf{R}_j - \mathbf{R}_i|) = e^2 \int d\mathbf{r} \int d\mathbf{r}' \frac{\psi^*_{\mathbf{R}_j}(\mathbf{r}) \psi_{\mathbf{R}_j}(\mathbf{r}') \psi^*_{\mathbf{R}_i}(\mathbf{r}') \psi_{\mathbf{R}_i}(\mathbf{r})}{|\mathbf{r}-\mathbf{r}'|}. \qquad (47)$$

For $R \gg l$,

$$J_{MZ}(R) \approx \frac{e^2}{R} \exp(-R^2/4l^2). \qquad (48)$$

This approximate expression for $J_{MZ}(R)$ is accurate to better than 5% even for neighboring sites over the range of Landau-level filling factors where the ground state is a Wigner crystal.

It is evident from Eq. (44) that if the ground state is approximated by the Maki-Zotos wave function, a ferromagnetic state in which all spins are parallel will be energetically favored. The energy increase when the relative orientation of spins on two sites separated by R changes from parallel to antiparallel is $J(R)$. For similar single-Slater-determinant variational wave functions at zero magnetic field, the tendency would be to favor antiferromagnetic orientations on neighboring sites,[6-8] except possibly when multisite ring exchanges become important. (Multisite ring exchanges are less important for the strong-magnetic-field Wigner crystal because magnetic confinement results in orbitals which are more strongly localized around lattice sites.) In the weak-field case, having opposite spins on neighboring sites reduces the kinetic energy density required by the Pauli exclusion principle in the region between the sites. In the strong-magnetic-field limit, the kinetic energy is quantized and is independent of the spin configuration so this mechanism favoring antiferromagnetism is not operative. Nevertheless, the Maki-Zotos wave function is a single Slater determinant and conclusions based upon its use should be examined critically. It is known, for example, that correlations can result in spin-singlet fluid ground states,[19] whereas the Hartree-Fock approximation would always predict ferromagnetic ground states. At zero magnetic field, the contribution from low-energy, long-wavelength phonon modes to the zero-point motion gives rise to long-range correlations which, for example, make the static structure factor vanish more quickly ($\propto q^{3/2}$) than it would for a system with short-range interactions. At strong magnetic field, even stronger correlations, which make the static structure factor vanish as q^2, result from the contribution to the zero-point motion of the collective cyclotron mode of all electrons. (In a Jastrow-Slater variational wave function such as that used by Zhu and Louie[8] the correlation factors would have to have a logarithmic spatial dependence in order to capture the correct long-distance ground-state correlations.) We cannot completely rule out on the basis of our calculations the possibility that correlations could invalidate our conclusion that the ground state is ferromagnetic. However, we consider this to be extremely unlikely.

B. Self-consistent Hartree-Fock calculations

One possible mechanism in favor of antiferromagnetism is the possibility of spreading the charge associated with a given lattice site more widely in the case of antiferromagnetic configurations, which could reduce the electrostatic energy. To probe the competition a little more deeply we have performed self-consistent Hartree-Fock calculations, based on the formalism of the previous section, comparing the energy of ferromagnetic and antiferromagnetic states on a square lattice. We now discuss the results of these calculations.

In the Hartree-Fock approximation, the spin order is unidirectional on a square lattice for both ferromagnetic and antiferromagnetic interactions. We choose a spin-quantization axis which is along the direction of the Zeeman coupling if one is present and is otherwise arbitrary. This allows us to set the order parameters which are off-diagonal in the spin indices to zero and simplify our calculation. Let a_0 be the lattice constant of the ferromagnetic square lattice with density $n = 1/a_0^2$ such that $2\pi n l^2 = \nu$. In the antiferromagnetic case we assume that the spin density is oppositely directed on the two sublattices [which have lattice constant $\sqrt{2} a_0$, and have a relative shift of $\mathbf{a} = \sqrt{2}(\frac{1}{2}, \frac{1}{2}) a_0$] so that

$$\langle \rho_{--}(\mathbf{G}) \rangle = e^{-i\mathbf{G} \cdot \mathbf{a}} \langle \rho_{++}(\mathbf{G}) \rangle \qquad (49)$$

where $\mathbf{G}$ is a *sublattice* reciprocal lattice vector. (We choose our coordinate system so that the primitive lattice vectors of the sublattice are along the Cartesian axes.) Equation (11) can again be simplified to a single equation:

$$(i\omega_n + \mu) G_{++}(\mathbf{G}, \omega_n) - \sum_{\mathbf{G}'} \tilde{F}(\mathbf{G}, \mathbf{G}') G_{++}(\mathbf{G}', \omega_n) = \delta_{\mathbf{G}, 0}, \qquad (50)$$

where

$$\tilde{F}(\mathbf{G}, \mathbf{G}') = \exp\left[\frac{1}{2} i\mathbf{G} \times \mathbf{G}' l^2\right] [(1 + e^{-i\mathbf{G} \cdot \mathbf{a}}) H(\mathbf{G}) - X(\mathbf{G})] \times \langle \rho_{++}(-\mathbf{G}) \rangle. \qquad (51)$$

The ground-state energy per particle becomes

$$E_{+-} = \frac{1}{\nu} \sum_{\mathbf{G}} \{H(\mathbf{G})[1 + \cos(\mathbf{G} \cdot \mathbf{a})] - X(\mathbf{G})\} |\langle \rho_{++}(\mathbf{G}) \rangle|^2. \qquad (52)$$

We have solved these equations self-consistently. Because of the variational nature of the Hartree-Fock approximation,

TABLE I. Energy of the square and triangular ferromagnetic states (SLF,TLF) and of the antiferromagnetic state on the square lattice (SLA) in the Hartree-Fock approximation in units of e^2/l. The relative energy difference between the ferromagnetic and antiferromagnetic states on the square lattice is given by ΔE_{spin} while the relative difference in energy between the ferromagnetic state on the triangular and square lattices is given by $\Delta E_{\mathrm{Coulomb}}$.

ν	E_{SLF}	E_{SLA}	E_{TLF}	ΔE_{spin} (%)	$\Delta E_{\mathrm{Coulomb}}$ (%)
1/3	-0.3857672	-0.3823134	-0.3884928	0.90	0.70
1/4	-0.3484399	-0.3478963	-0.3511452	0.16	0.77
1/5	-0.3196321	-0.3195124	-0.3219969	0.037	0.73
1/6	-0.2964916	-0.2964471	-0.2985717	0.015	0.70
1/7	-0.2775104	-0.2774874	-0.2793787	0.0083	0.67
1/8	-0.2616473	-0.2616346	-0.2633555	0.0049	0.65
1/10	-0.2365415	-0.2365379	-0.2380218	0.0015	0.62

TABLE II. Energy of the square and triangular ferromagnetic states (SLF,TLF) and of the antiferromagnetic state on the square lattice (SLA) in the Maki-Zotos approximation in units of e^2/l. The relative energy difference between the ferromagnetic and antiferromagnetic states on the square lattice is given by ΔE_{spin} while the relative difference in energy between the ferromagnetic state on the triangular and square lattices is given by $\Delta E_{\mathrm{Coulomb}}$.

ν	E_{SLF}	E_{SLA}	E_{TLF}	ΔE_{spin} (%)	$\Delta E_{\mathrm{Coulomb}}$ (%)
1/3	-0.3858614	-0.3814086	-0.3885208	1.15	0.68
1/4	-0.3482640	-0.3474804	-0.3511413	0.23	0.82
1/5	-0.3194893	-0.3193454	-0.3219900	0.045	0.78
1/6	-0.2964083	-0.2963812	-0.2985680	0.0091	0.72
1/7	-0.2774646	-0.2774594	-0.2793770	0.0019	0.68
1/8	-0.2616223	-0.2616213	-0.2633548	0.00038	0.66
1/10	-0.2365341	-0.2365340	-0.2380216	0.000016	0.63

these solutions provide us with the lowest-energy single Slater determinant consistent with the assumed magnetic and translational broken symmetry. In particular, the solutions to these equations will always give a lower energy than the energy for the corresponding Maki-Zotos wave function. The optimization process implicit in obtaining a self-consistent solution of the Hartree-Fock equations results in cyclotron orbits on each lattice site which are distorted by their average environments, including their magnetic environments, in a way which minimizes the total interaction energy. It is still true, however, that the cyclotron orbits on different sites are not correlated with each other. The error introduced as a consequence can be estimated by using a harmonic approximation for the strong-field Wigner crystal, which is reasonably accurate from an energetic point of view throughout the regime where the ground state is an electron crystal. In the harmonic approximation the many-body Schrödinger equation can be solved exactly and the ground-state energy is the sum of the classical Madelung energy and the quantum zero-point energy, i.e.,

$$E_{\mathrm{harmonic}} = -0.78213\nu^{1/2} + 0.24101\nu^{3/2}, \qquad (53)$$

for the hexagonal lattice. The Hartree-Fock approximation describes the Madelung term exactly (in the limit $\nu \to 0$, the HFA energy coincides with the classical energy of a point lattice) and overestimates[20] the zero-point energy by approximately 25% (at $\nu = 0.2$).

The results of our calculations are summarized in Tables I and II. In Table I, we list the ground-state energy per electron in the HFA for the square lattice antiferromagnetic (SLA) and ferromagnetic (SLF) states as well as for the triangular lattice ferromagnetic (TLF) state. Table II contains a similar calculation using a simplified form of the Maki and Zotos wave function where we have neglected the overlapping between two wave functions centered on different sites so that the single-electron density can be approximated by

$$\langle n(\mathbf{r}) \rangle = \sum_i |\psi_{\mathbf{R}_i}(\mathbf{r})|^2 = \frac{1}{2\pi l^2} \sum_i e^{-(\mathbf{r}-\mathbf{R}_i)^2/2l^2}, \quad (54)$$

or, equivalently, in the ferromagnetic case

$$\langle \rho(\mathbf{G}) \rangle_{\mathrm{MZ}} = \nu e^{-G^2 l^2/4}. \qquad (55)$$

(For the SLA case, $\nu \to \nu/2$ and the $\mathbf{G}$'s are replaced by the sublattice reciprocal lattice vectors.) We use the order parameters defined by Eq. (55) in Eq. (28) to compute the Maki-Zotos ground-state energies tabulated in Table II. We remark that this procedure is exactly equivalent to computing Eq. (44) (when the interaction with a positive homogeneous background of charges is added to this last equation). Note also that these results include only the Coulomb energy. These tables report also the results of calculations performed for filling factors where the ground state is *not* believed to be a Wigner crystal. These large-ν results are intended to illustrate trends in the self-consistent Hartree-Fock approximation solutions and not to be physically realistic.[21] In order to obtain a stable Wigner crystal state in the Hartree-Fock approximation and to get a convergent result for its ground-state energy, we need to consider a large number of order parameters or, equivalently, of reciprocal lattice vectors (RLV's). The number of RLV's to be considered increases as the filling factor gets small and at some point, the calculation becomes numerically prohibitive. Moreover, the number of RLV's that has to be taken into account is bigger for the antiferromagnetic lattice than in the ferromagnetic lattice since the antiferromagnetic lattice with filling factor ν is made of two sublattices with filling factor $\nu/2$. Typically, while 100 RLV's is sufficient to obtain the ground-state energy for filling factors around $\nu = 1/3$ in the ferromagnetic case, we need to consider about 800 RLV's to obtain the ground-state energy to the accuracy reported in Table I (accuracy which is necessary for comparison with the Maki-Zotos energy), for filling factor $\nu = 1/10$ in the antiferromagnetic lattice.

We see that for the larger filling factors, the difference in energy between Hartree-Fock square lattice ferromagnetic and antiferromagnetic states, $\Delta E_{\mathrm{spin}} = (E_{\mathrm{SLF}} - E_{\mathrm{SLA}})/E_{\mathrm{SLF}}$, agrees quite closely with what would be predicted by the Maki-Zotos wave function [Eq. (55)]. At smaller filling factors, however, the Hartree-Fock energy difference between

TABLE III. Value of the exchange integral, in units of e^2/l, on the square lattice obtained from various approximations: J_{MZ} is from the definition of the exchange integral given in Eq. (60), J_{HFA} is obtained from the energy difference between the ferromagnetic and antiferromagnetic states [Eq. (59)], and J_{TDHFA} is obtained by fitting the TDHFA spin-wave dispersion relation with the spin-wave dispersion relation of the Heisenberg model (see text).

ν	J_{MZ}	J_{HFA}	J_{TDHFA}
1/3	0.22×10^{-2}	0.17×10^{-2}	0.13×10^{-2}
1/4	0.39×10^{-3}	0.27×10^{-3}	0.24×10^{-3}
1/5	0.72×10^{-4}	0.60×10^{-4}	0.43×10^{-4}
1/6	0.14×10^{-4}	0.22×10^{-4}	
1/7	0.26×10^{-5}	0.11×10^{-4}	
1/8	0.50×10^{-6}	0.63×10^{-5}	
1/10	0.19×10^{-7}	0.18×10^{-5}	

these two spin states is much bigger than what would be predicted by the Maki-Zotos wave function. The energy reduction due to the added variational freedom compared to the Maki-Zotos wave function is larger for the ferromagnetic state than for the antiferromagnetic state and this leads to an increased energy difference between the two states. [See also Table III where, as discussed below, J_{MZ} is proportional to $(E_{SLF} - E_{SLA})$ evaluated with the Maki-Zotos wave function and J_{HFA} is proportional to $(E_{SLF} - E_{SLA})$ evaluated in the HFA.[22]] In both the Makis-Zotos and HF approximations, the ferromagnetic state has the lowest energy. In Fig. 1, we plot the *difference* in density: $\langle n(\mathbf{r}) \rangle_{HFA} - \langle n(\mathbf{r}) \rangle_{MZ}$ for the SLF and SLA at filling factor $\nu = 1/8$. It is clear from this figure that the HFA minimizes the Coulomb energy in both the SLF and SLA cases by removing charges along the direction of the nearest-neighbor sites and putting them along the direction of the next-nearest-neighbor sites. This is just what we expect at such a small filling factor, where overlap between wave functions on different sites is very small and the ground-state energy is dominated by the (direct) Coulomb interaction. According to our calculations more charge redistribution occurs in the ferromagnetic case. For the triangular lattice, a similar calculation gives a much smaller difference in densities, reflecting a loss in the variational freedom due to the higher coordination number of the triangular lattice.

We remark that similar self-consistent calculations for a single-band Hubbard model at half filling would find the antiferromagnetic state to be lower in energy, correctly reflecting the superexchange coupling in that system.[23] We also see that, as anticipated above, the difference between the square lattice ferromagnetic state and the triangular lattice ferromagnetic state energy, $\Delta E_{Coulomb} = (E_{TLF} - E_{SLF})/E_{TLF}$, is much larger than the difference between ferromagnetic and antiferromagnetic states on the same lattice. This energy difference is almost constant over the range of filling factors considered here, decreasing slowly as ν decreases. For $\nu \to 0$, $\Delta E_{Coulomb}$ approaches its Madelung energy value, 0.53%.[12]

IV. COLLECTIVE MODE CALCULATIONS

As we described above, the ground-state order parameters can be used to calculate the spin-wave collective modes. In
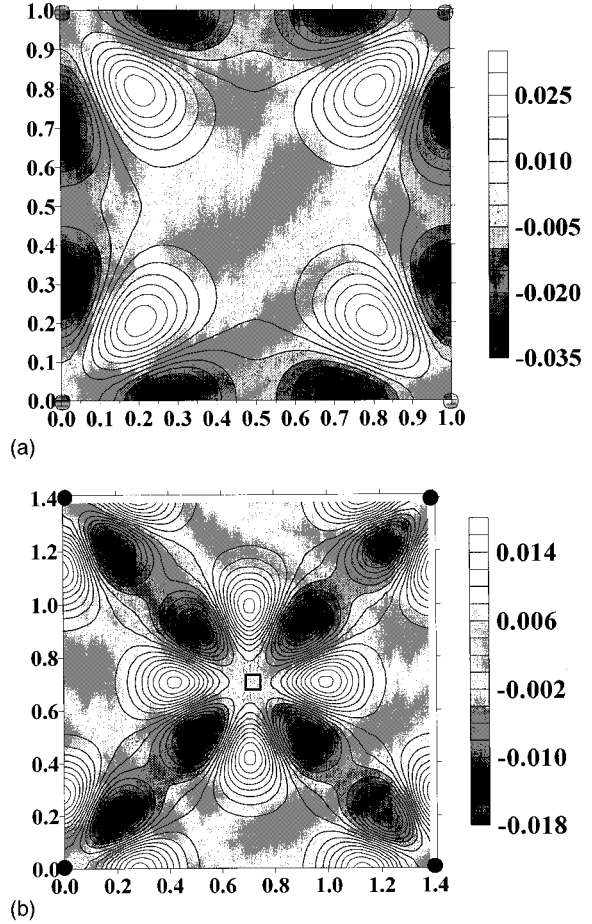

FIG. 1. Difference in densities between the Hartree-Fock and Maki-Zotos approximations at filling factor $\nu = 1/8$ and in units of $1/a_0^2$ for (a) the ferromagnetic square lattice and (b) the antiferromagnetic square lattice. For the ferromagnetic state, the lattice sites are indicated by gray circles. For the antiferromagnetic state, sites on one sublattice are indicated by black circles and sites on the other sublattice are indicated by empty squares. Note that the orientation of the lattice differs in (a) and (b).

the ferromagnetic ground state, we showed that the density response function χ^{nn}, or equivalently the longitudinal spin response function $\chi^{zz} = \chi^{nn}/4$, is uncoupled from the transverse spin response function χ^{+-}. The poles of the longitudinal spin response function are nothing but the phonons of the Wigner crystal for which we have already computed the dispersion relation in Ref. 9. The transverse spin excitations are the magnon collective modes of the ferromagnetic Wigner crystal. Figs. 2 and 3 show the TDHFA dispersion relations for the SF and TF lattices, respectively, at different values of the filling factor. [When the electronic g factor is nonzero all magnon collective modes energies are increased by the Zeeman gap $g^* \mu_B B$. In the simple collinear states (SLF, SLA, and TLF) that we consider here, a small Zeeman term has no effect on the calculation of the order parameters.] We remark that, because of the numerical approach used in this work, it is not possible to obtain the dispersion relations at very small filling factors without having to consider a prohibitively large number of reciprocal lattice vectors. For the square lattice, we were not able to obtain accurate results for $\nu < 1/5$ while for the triangular lattice $\nu = 1/7$ was the lower limit.
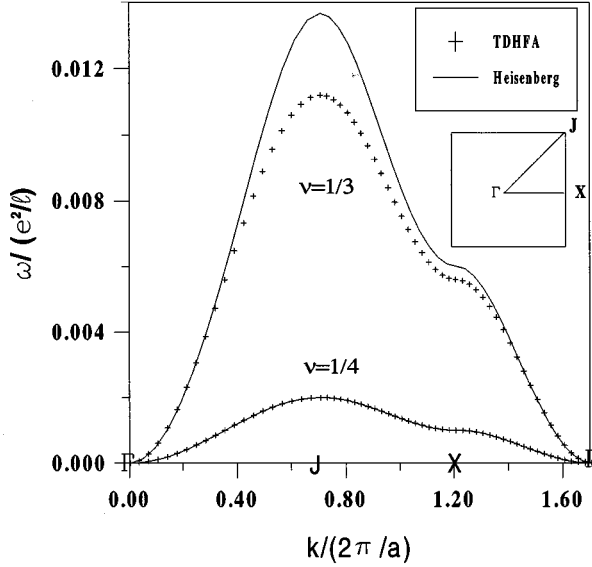
FIG. 2. Dispersion relation of the spin waves of the ferromagnetic square lattice obtained from the TDHFA and from the Heisenberg model at different filling factors. The dispersion relation is plotted along the edges of the irreducible Brillouin zone (shown in inset) of the square lattice with lattice spacing a. In units of $2\pi/a$, $\Gamma = (0,0)$, $J = (1/2,1/2)$, and $X = (1/2,0)$.

It is interesting to compare these magnon dispersion relations with the dispersion relation of the spin waves of the Heisenberg model where the spins are localized on the lattice sites and the Hamiltonian is given by

$$H = -J \sum_{i\,\boldsymbol{\delta}} \mathbf{S}_i \cdot \mathbf{S}_{i+\boldsymbol{\delta}}. \qquad (56)$$
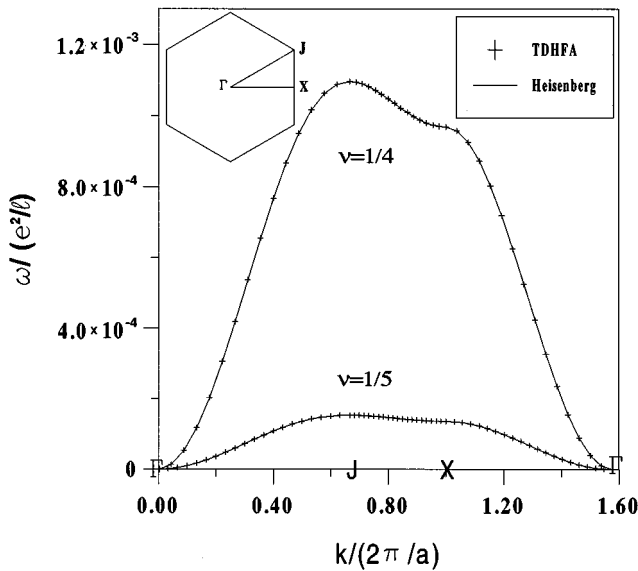

FIG. 3. Dispersion relation of the spin waves of the ferromagnetic triangular lattice obtained from the TDHFA and from the Heisenberg model at different filling factors. The dispersion relation is plotted along the edges of the irreducible Brillouin zone (shown in inset) of the triangular lattice with lattice spacing a. In units of $2\pi/a$, $\Gamma = (0,0)$, $J = (1/\sqrt{3},1/3)$, and $X = (1/\sqrt{3},0)$.

TABLE IV. Value of the exchange integral, in units of e^2/l, on the triangular lattice obtained from the various approximations described in Table III.

ν	J_{MZ}	J_{TDHFA}
1/3	0.99×10^{-3}	0.74×10^{-3}
1/4	0.14×10^{-3}	0.12×10^{-3}
1/5	0.20×10^{-4}	0.17×10^{-4}
1/6	0.29×10^{-5}	0.25×10^{-5}
1/7	0.44×10^{-6}	0.40×10^{-6}
1/8	0.67×10^{-7}	
1/10	0.16×10^{-8}	

(The summation is over the lattices sites i and the ν_0 nearest neighbors of the lattice. Note that this convention for the exchange constant results in double counting each neighbor pair.) In that case,

$$\omega(\mathbf{k}) = 2J\nu_0 s(1 - \gamma_{\mathbf{k}}), \qquad (57)$$

with

$$\gamma_{\mathbf{k}} = \frac{1}{\nu_0} \sum_{\boldsymbol{\delta}} e^{i\mathbf{k}\cdot\mathbf{R}_\delta}, \qquad (58)$$

and $s = 1/2$.

The solid lines in Figs. 2 and 3 show the dispersion relation obtained from a nearest-neighbor interaction Heisenberg model with the interaction strength chosen to reproduce the TDHFA numerical results. The fit is quite good and becomes almost perfect at smaller filling factors. (The discrepancy at $\nu = 1/3$ can be improved by fitting with nonzero next-nearest-neighbor coupling.) The exchange integral J_{TDHFA} obtained in this way from the TDHFA dispersion relation, for different filling factors, is listed in Table III (square lattice) and Table IV (triangular lattice). These tables also show values of the exchange integral calculated in two other ways. From Table I, we see that the ground-state energy is minimal for the polarized square lattice. We can estimate the strength of the exchange coupling from this energy difference as follows. We assume that, as far as the magnetic degrees of freedom are concerned, the Hartree-Fock solution yields an Ising approximation to the antiferromagnetic ground state, i.e., it does not capture the quantum fluctuations which would be present in a true antiferromagnetic ground state. It is then easy to see[24] that, for the square lattice,

$$J_{HFA} = \frac{E_{SLA} - E_{SLF}}{2}. \qquad (59)$$

This expression assumes that non-nearest-neighbor exchange coupling is negligible. (Note that a similar calculation is not possible for the triangular lattice because of frustration.) We can also compute the exchange integral directly from the Maki-Zotos wave function expression, Eq. (47). This gives Eq. (45) or, using $2\pi nl^2 = \nu$ with $n = 1/\alpha a_0^2$ [$\alpha = 1$ (SF) or $\alpha = \sqrt{3}/2$ (TF)],

$$J_{\mathrm{MZ}}=\left(\frac{e^2}{l}\right)\left(\frac{\pi}{4}\right)^{1/2}e^{-3\pi/4\alpha\nu}I_0\left(\frac{\pi}{4\alpha\nu}\right). \qquad (60)$$

Note that if the Maki-Zotos energies are used in Eq. (59) instead of the HFA energies, J_{MZ} is recovered exactly as long as non-nearest-neighbor interactions are negligible.

For the TLF, the exchange integral obtained from the TDHFA is only slightly smaller than J_{MZ}. For the square lattice, the exchange integral obtained from the TDHFA is smaller than both J_{MZ} and the HFA value over the range of ν where we are able to complete calculations. At smaller filling factors, since the difference between the two spin states decreases faster with the Maki-Zotos wave function than with the HFA, the HF value of J is much larger than the Maki-Zotos value. We expect the TDHFA result to remain close to the HFA result in this regime. Unfortunately, we cannot check this assumption numerically since we cannot compute the TDHFA value of J at smaller filling factor (the matrix size becomes prohibitively large). However, since the TDHFA is obtained from a functional differentiation of the HFA, our assumption seems reasonable. In any case, the present result shows clearly that, in the Wigner crystal, the interaction between spins, at small filling factor, is mainly from nearest neighbors.

In the small-wave-vector limit, the Heisenberg dispersion relation on the triangular lattice is given by $\omega(k)=\frac{3}{2}J(ka_0)^2\equiv D(kl)^2$ where $D=2\pi\sqrt{3}J/\nu$ in units of e^2/l. With J given by J_{TDHFA} as calculated above, we find that $D=0.024$ at $\nu=1/3$ and $D=9.3\times10^{-3}$ at $\nu=1/5$. These values should be compared with those of the liquid state where $D=4\pi l^2\rho_s/\nu$ where ρ_s is the spin stiffness. For the liquid state it is possible to express the spin stiffness in terms of the pair correlation function[19,25] and this has been evaluated using a hypernetted-chain approximation for the liquid-state pair correlation function in Ref. 25. For the liquid state we find that $D=0.035(e^2/l)$ at $\nu=1/3$ and $D=0.015(e^2/l)$ at $\nu=1/5$. We see that the spin stiffness is larger for the liquid state and increasingly so as the filling factor decreases. This result is consistent with the view of the strongly correlated electron states as quantum melted crystals of electrons whose size is smeared on a magnetic length scale by rapid cyclotron motion. When long-range order is lost, the cyclo-tron orbits will overlap more strongly on average and the relative spin orientation of nearby electrons will assume a larger importance.

V. SUMMARY

In the strong-magnetic-field limit, we have argued that the lowest-energy spin state of the Wigner crystal is the ferromagnetic state. Our conclusion is based in part on a comparison of ferromagnetic and antiferromagnetic state energies of square lattice Wigner crystal states calculated in the Hartree-Fock approximation and in part on the observation that the superexchange mechanism, which tends to favor antiferromagnetism, is absent in the strong-magnetic-field limit. The spin-wave dispersion relations, which we compute in the TDHFA, show that the ferromagnetic lattice is stable at filling factors where crystallization occurs. In this limit, the interactions between spins on the lattice are dominated by nearest-neighbor exchange coupling. Our results appear to show that small distortions of the wave functions for electrons on one lattice site, due to their interactions with electrons on nearby lattice sites, are responsible for a large relative increase in the small exchange couplings at small filling factors. A comparison with the liquid state at filling factors $\nu=1/3$ and $\nu=1/5$ shows that the spin stiffness of the ferromagnetic liquid states which occur at these fillings is substantially larger than that of corresponding crystal states. In closing we remark that the recent sucessful application[26] of nuclear-magnetic-resonance methods to two-dimensional electron systems, suggests that the magnetic properties of two-dimensional electron systems in the regime where the Wigner crystal state occurs will soon be open to experimental investigation, so that our conclusions can be tested. These experiments should open up a host of interesting new questions, related to disorder and thermal fluctuations.

ACKNOWLEDGMENTS

[1] E.P. Wigner, Phys. Rev. **46**, 1002 (1934).

[2] For a series of reviews of recent experimental and theoretical work focusing on two-dimensional electrons at strong magnetic fields, see *Physics of the Electron Solid*, edited by S.T. Chui (International Press, Boston, 1994).

[3] We will imagine that a magnetic field, if present, couples only to the orbital electronic degrees of freedom. This situation is frequently close to being realized for electrons in semiconductors where the g factor is often small.

[4] It is frequently possible to tune the g factor to zero by applying pressure or, in the case of two-dimensional electrons, by adjusting quantum well widths. See, for example, M. Dobers, K. v. Klitzing, and G. Weimann, Phys. Rev. B **38**, 5453 (1988); G. Lommer, F. Malcher, and U. Rössler, Phys. Rev. Lett. **60**, 728 (1988); N.G. Morawicz, K.W.J. Barnham, A. Briggs,

C.T. Foxon, J.J. Harris, S.P. Najda, J.C. Portal, and M.L. Williams, Semicond. Sci. Technol. **8**, 333 (1993); M. Cardona, N.E. Christensen, and G. Fasol, Phys. Rev. B **38**, 1806 (1988).

[5] C. Herring, in *Magnetism*, edited by C.I. Rado and H. Suhl (Academic, London, 1966), Vol. IV, Chap. 4.

[6] D.J. Thouless, Proc. Phys. Soc. London **86**, 893 (1965).

[7] D. Ceperley, Phys. Rev. B **18**, 3126 (1978); B. Tanatar and D.M. Ceperley, *ibid.* **39**, 5005 (1989).

[8] Xuejun Zhu and Steven G. Louie, Phys. Rev. B **48**, 13 661 (1993); (unpublished).

[9] R. Côté and A.H. MacDonald, Phys. Rev. Lett. **65** , 2662 (1990); Phys. Rev. B **44**, 8759 (1991).

[10] R. Côté, L. Brey, and A.H. MacDonald, Phys. Rev. B **46**, 10 239 (1992); H.A. Fertig, R. Côté, A.H. MacDonald, and S. Das

Sarma, Phys. Rev. Lett. **69**, 816 (1992); H.A. Fertig and R. Côté, Phys. Rev. B **48**, 2391 (1993); R. Côté and H.A. Fertig, *ibid.* **48**, 10955 (1993); R. Côté, L. Brey, H.A. Fertig, and A.H. Mac-Donald, *ibid.* **51**, 13 475 (1995);

[11] X.M. Chen and J.J. Quinn, Phys. Rev. B **45**, 11 054 (1992); **47**, 3999 (1993); L. Zheng and H.A. Fertig (unpublished).

[12] L. Bonsall and A.A. Maradudin, Phys. Rev. B **15**, 1959 (1977).

[13] For early work on the Hartree-Fock approximation for two-dimensional electron systems in the strong-magnetic-field limit, see H. Fukuyama, P.M. Platzman, and P.W. Anderson, Phys. Rev. B **19**, 5211 (1979); R.R. Gerhardts and Y. Kuramoto, Z. Phys. B **44**, 301 (1981); A.H. MacDonald and D.B. Murray, Phys. Rev. B **32**, 2291 (1985).

[14] By particle-hole symmetry the ground state in the strong-magnetic-field limit will also be a Wigner crystal state through most of the filling factor interval $1.73 < \nu < 2$. Interesting broken translational symmetry states (Skyrme crystals), whose detailed properties are quite sensitive to the g factor, also occur for ν near 1: L. Brey, H.A. Fertig, R. Côté, and A.H. MacDonald, Phys. Rev. Lett. **75**, 2562 (1995). Our attention here is limited to the Wigner crystal case.

[15] R.R.P. Singh and D.A. Huse, Phys. Rev. Lett. **68**, 1766 (1992).

[16] K. Maki and X. Zotos, Phys. Rev. B **28**, 4349 (1983).

[17] We choose the symmetric gauge here to facilitate comparisons with the work of Maki and Zotos.

[18] The nonorthogonality correction to the exchange energy for electrons centered by R is $\propto \exp(-R^2/2l^2)$ while the exchange energy is $\propto \exp(-R^2/4l^2)$.

[19] M. Rasolt and A.H. MacDonald, Phys. Rev. **34**, 5530 (1986).

[20] See, for example, A.H. MacDonald, in *Low-Dimensional Electronic Systems*, edited by G. Bauer, F. Kuchar, and H. Heinrich (Springer-Verlag, Berlin, 1992).

[21] For the square lattice ferromagnetic case, the $\nu = 1/3$ Maki-Zotos energy is slightly *lower* than the corresponding Hartree-Fock approximation ground-state energy because of our neglect of effects associated with the nonorthogonality and overlapping of orbitals on different lattice sites. These corrections quickly become negligible at smaller filling factors.

[22] We note that, in computing ΔE_{spin} for $\nu = 1/10$, we have kept more than the seven digits indicated in Tables I and II.

[23] See, for example, G. Vignale and M.R. Hedayati, Phys. Rev. B **42**, 786 (1990).

[24] O. Madelung, *Introduction to Solid-State Theory* (Springer-Verlag, Berlin, 1981), pp. 156–162.

[25] K. Moon *et al.*, Phys. Rev. B **51**, 5138 (1995) (see p. 5145).

[26] S.E. Barrett, G. Dabbagh, L.N. Pfeiffer, K.W. West, and R. Tycko, Phys. Rev. Lett. **74**, 5112 (1995); R. Tycko, S.E. Barrett, G. Dabbagh, L.N. Pfeiffer, and K.W. West, Science **268**, 1460 (1995).